



# CHORUS

This is the accepted manuscript made available via CHORUS. The article has been published as:

## Viscous damping of r-modes: Large amplitude saturation

Mark G. Alford, Simin Mahmoodifar, and Kai Schwenzer

Phys. Rev. D **85**, 044051 — Published 22 February 2012

DOI: [10.1103/PhysRevD.85.044051](https://doi.org/10.1103/PhysRevD.85.044051)

# Viscous damping of r-modes: Large amplitude saturation

Mark G. Alford, Simin Mahmoodifar and Kai Schwenzer

*Department of Physics, Washington University, St. Louis, Missouri, 63130, USA*

We analyze the viscous damping of r-mode oscillations of compact stars, taking into account non-linear viscous effects in the large-amplitude regime. The qualitatively different cases of hadronic stars, strange quark stars, and hybrid stars are studied. We calculate the viscous damping times of r-modes, obtaining numerical results and also general approximate analytic expressions that explicitly exhibit the dependence on the parameters that are relevant for a future spindown evolution calculation. The strongly enhanced damping of large amplitude oscillations leads to damping times that are considerably lower than those obtained when the amplitude dependence of the viscosity is neglected. Consequently, large-amplitude viscous damping competes with the gravitational instability at all physical frequencies and could stop the r-mode growth in case this is not done before by non-linear hydrodynamic mechanisms.

## I. INTRODUCTION

A compact star is one of the most stable forms of matter in the universe. The only instability that threatens its existence is collapse into a black hole, triggered by unstable radial oscillation modes that push the star below its Schwarzschild radius. However, there are other unstable oscillation modes, the so called r-modes [1, 2], which damp the rotation of the star by the emission of gravitational radiation [3]. In slowly-rotating stars r-modes themselves are damped by bulk and shear viscosity, but at high rotation frequencies they are unstable and grow exponentially. In a companion paper [4] we analyzed these instability regions in detail. The main result of that study was that these regions vary greatly between qualitatively different classes of stars containing distinct phases of strongly interacting matter, but are extremely insensitive to unknown quantitative details of the equation of state and the transport properties within a given class. Therefore, a proper understanding of the r-mode dynamics could in the future provide robust signatures for the presence of exotic phases in compact stars.

Since exponentially growing r-modes will destroy the star if their growth is not stopped by some non-linear mechanism, the fact that fast spinning compact stars are observed suggests that such a non-linear damping mechanism is indeed present. More importantly, even if stopped at a finite amplitude, r-modes still strongly emit gravitational waves and could provide an extremely efficient mechanism for the spin-down of compact stars [5] and an interesting signal for terrestrial gravitational wave detectors. Spin-down due to r-modes could explain the observed absence of fast-spinning young stars despite the fact that their creation during a supernova could naturally lead to a fast spinning remnant. For spin-down via r-modes the size of the saturation amplitude is crucial. If the amplitude  $\alpha$  is too low, it takes too long to spin down the star; if the amplitude is too large,  $\alpha > O(1)$ , the r-mode would disrupt the star's structure, and even before this point the r-mode could be destroyed. If the r-mode amplitude saturates at an intermediate value, a fast spin-down is possible. Previously, various mechanisms for the

large-amplitude behavior of r-modes have been suggested [6]. They include the coupling between different modes [7, 8], the decay into daughter modes and the eventual transformation of the r-mode energy into differential rotation [9, 10], friction between different layers of the star, and surface effects in the star's crust [11].

Here we study an alternative mechanism that does not involve such complicated non-linear dynamical or structural effects. It is present already in a standard hydrodynamical description and exploits the fact that at large amplitudes the damping due to bulk viscosity increases dramatically with the amplitude [12–15]. In this suprathreshold regime, where the deviation from chemical equilibrium  $\mu_\Delta$  fulfills  $\mu_\Delta \gtrsim T$ , the viscous damping could overcome the initial gravitational instability and saturate the r-mode. However, as shown in [12], the bulk viscosity has a maximum as a function of the amplitude and decreases again at even larger amplitudes. If the amplitude exceeds this critical value then the r-mode growth cannot be stopped by viscous damping and other non-linear dynamic effects [6–10] are required to saturate it. Nevertheless, we find that over a significant region of the parameter space the suprathreshold enhancement is indeed sufficient to saturate the r-mode at a finite amplitude and the r-mode can then efficiently spin down the star. This is in contrast to certain non-linear hydrodynamical effects where the r-mode could completely decay [10] and would not be able to cause an appreciable spin-down of the star.

For r-modes with amplitudes sufficiently below the maximum, we give general analytic expressions for the suprathreshold damping time valid for various forms of dense matter. For r-modes with arbitrary amplitudes, where an analytic evaluation is not possible, we give a general expression for the bulk viscosity damping time that includes the complete parameter dependence required for the analysis of the star's evolution, encoded in a two-parameter function that can be numerically computed and tabulated for different star models. This offers an explicit framework for the consistent inclusion of the r-mode saturation into a star evolution analysis and supersedes previously necessary model assumptions [5]. We will analyze the same star models as in our recent

companion paper [4] and thereby extend this study to the suprathermal regime. These include neutron stars, hybrid stars and strange stars. In addition, motivated by the recent observation of a  $2M_\odot$  star [16, 17] we only study models that also yield heavy stars. Moreover, similar to the analytic results in [4], we give approximate analytic expressions for the maximum saturation amplitude that exhibit the detailed parameter dependence on the equation of state and the transport properties of dense matter. In addition to the standard fundamental  $m=2$  r-mode we also study the saturation of higher multipoles and find that they saturate at significantly lower amplitudes. In this work we concentrate on the effects of suprathermal bulk viscosity on the damping times [18] and the suitably extended concept of the instability regions, and defer a comprehensive analysis of the star evolution to future work.

## II. DAMPING OF STAR OSCILLATIONS

In this section we discuss the prerequisites needed for the analysis of compact star oscillations and their damping. In particular we discuss the large amplitude enhancement of the bulk viscosity which will provide a mechanism for the saturation of r-modes. This topic had been studied in [12] and we refer the reader to this work for further details. The analysis further requires the stable equilibrium configuration of the star and the r-mode profile. These have been discussed in more detail in our companion article on the damping of small amplitude r-modes [4] and we will here only briefly recall these results.

### A. Suprathermal viscosity

The bulk viscosity describes the local dissipation of energy in a fluid element in one cycle of compression and rarefaction, driven by some oscillation mode of the star. The integration over the whole star yields the corresponding total energy dissipation of an oscillation mode as will be discussed in section III. Recently the bulk viscosity of large-amplitude oscillations has been studied in detail in [12], which builds on the classic work [14] and provides general expressions valid for various forms of matter and arbitrary equations of state.

Bulk viscosity is generally induced by slow weak-interaction processes whose rate takes the parametric form

$$\Gamma^{(\leftrightarrow)} = -\tilde{\Gamma}T^\delta \mu_\Delta \left( 1 + \sum_{j=1}^N \chi_j \left( \frac{\mu_\Delta^2}{T^2} \right)^j \right), \quad (1)$$

where  $T$  is the temperature and  $\mu_\Delta$  represents the quantity that is driven out of equilibrium due to the oscillations and its re-equilibration leads to the bulk viscosity.

The latter is given by the difference of the sums of chemical potentials of the particles in the initial and final state of the relevant weak process. The  $\chi_j$  are coefficients that characterize the non-linear (large amplitude) contribution to the re-equilibration rate. The series terminates at a finite order  $N$  which is determined by the number and type of particles in the initial and final states of the dominant re-equilibration process and is connected to the temperature dependence via  $\delta=2N$ .

As has been shown in [12] the bulk viscosity can be written in a general form that expresses its full underlying parameter dependence in terms of the coefficients  $d$  of the driving term and  $f$  of the feedback term

$$d \equiv \frac{C}{T} \frac{\Delta n}{\bar{n}}, \quad f \equiv \frac{B\tilde{\Gamma}T^\delta}{\omega},$$

in the differential equation that determines the oscillation  $\mu_\Delta$ . These expressions depend on the oscillation frequency  $\omega$ , the conserved number density fluctuation  $\Delta n/\bar{n}$ , as well as the susceptibilities

$$C \equiv \bar{n} \left. \frac{\partial \mu_\Delta}{\partial n} \right|_x, \quad B \equiv \frac{1}{\bar{n}} \left. \frac{\partial \mu_\Delta}{\partial x} \right|_n, \quad (2)$$

with respect to the density  $n$  and the fraction  $x$  of a particular particle that is driven out of equilibrium. The general result can be parameterized in the form [12]

$$\zeta = \zeta_{max}^< \mathcal{I}(d, f), \quad (3)$$

where the global maximum of the viscosity

$$\zeta_{max}^< = \frac{C^2}{2\omega B}$$

is taken at

$$d = 0, f = 1 \quad \Rightarrow \quad T_{max} = \left( \frac{\omega}{\tilde{\Gamma}B} \right)^{\frac{1}{\delta}} \quad (4)$$

and the non-trivial dimensionless integral

$$\mathcal{I}(d, f) \equiv \frac{2}{\pi T d} \int_0^{2\pi} \mu_\Delta(\varphi; d, f) \cos(\varphi) d\varphi \quad (5)$$

has to be tabulated for each considered form of matter with a particular dominant weak re-equilibration process. Since both  $d$  and  $f$  depend on the temperature and the required parameter regions are therefore non-trivial, see [19], this is most conveniently done in terms of the new variable  $\tilde{d} \equiv d f^{1/\delta}$  for the function  $\tilde{\mathcal{I}}(\tilde{d}, f) = \mathcal{I}(d, f)$ . This form of the bulk viscosity is crucial for the study of damping times below, which involve an integration over

the whole star, and therefore requires the complete density and amplitude dependence of the viscosity in addition to the temperature and frequency dependence which are used in standard analyses.

In general the bulk viscosity features three distinct characteristic regions. Almost all previous analyses of r-mode damping have been limited to the *subthermal* regime  $\mu_\Delta \ll T$ , where  $\mu_\Delta$  is linear in  $d \sim \Delta n$ , so the viscosity is independent of the amplitude and has the analytic form

$$\zeta^< = \zeta_{max}^< \frac{2f}{1+f^2} = \frac{C^2 \tilde{\Gamma} T^\delta}{\omega^2 + (B \tilde{\Gamma} T^\delta)^2} \quad (6)$$

Yet, since the r-mode is unstable and rises exponentially it eventually reaches the *suprathermal regime*  $\mu_\Delta \gtrsim T$  which will be studied below. This regime is divided into two qualitatively different parts. In an intermediate regime  $\mu_\Delta$  is still linear in  $d$  but the viscosity strongly rises. For  $f \ll 1$  this part allows an analytic solution given by

$$\begin{aligned} \zeta^\sim &= \zeta_{max}^< f d^{2j} \sum_{j=0}^N \frac{(2j+1)!! \chi_j}{2^{j-1} (j+1)!} \\ &= \frac{C^2 \tilde{\Gamma} T^\delta}{\omega^2} \left( 1 + \sum_{j=1}^N \frac{(2j+1)!! \chi_j}{2^j (j+1)!} \left( \frac{C \Delta n}{T \bar{n}} \right)^{2j} \right) \end{aligned} \quad (7)$$

which can be combined with the subthermal result to give an approximate analytic solution for both regions  $\zeta^\gtrsim = \zeta^< + \theta(T - T_{max}) \zeta^\sim$ . At even higher amplitudes the rise of  $\mu_\Delta$  becomes weaker due to non-linear saturation effects so that the viscosity has a maximum and decreases again. In the asymptotic limit  $\mu_\Delta \gg T$ , the viscosity scales as

$$\zeta \sim \left( \frac{\Delta n}{\bar{n}} \right)^{-\frac{2N}{2N+1}}. \quad (8)$$

As discussed in appendix B, for the special case of strange quark matter an approximate analytic result is possible that includes this large amplitude regime.

In contrast to the bulk viscosity, the shear viscosity of dense matter is independent of the frequency and amplitude of an external oscillation and over certain temperature ranges its dependence on temperature is approximately a simple power law. Shear viscosity becomes large at low temperatures and therefore it is the dominant process for damping of the r-modes of cooler stars. Correspondingly we can parameterize the shear viscosity as

$$\eta = \tilde{\eta} T^{-\sigma} \quad (9)$$

by simply factoring out the temperature dependence with exponent  $\sigma$ .

## B. Star models

We study in this work the same model examples of compact stars as in our companion paper [4]. These include neutron stars, strange stars [20], and hybrid stars, and we consider in each case a star with a standard mass of  $1.4 M_\odot$  and a heavy star with a mass of  $2 M_\odot$ . For the neutron stars we use nuclear matter obeying the APR equation of state [21] and as a low density extension of the APR data we use [22, 23]. In order to apply our general results to other equations of state, away from chemical equilibrium we use the simple quadratic parameterization in terms of the symmetry energy employed in [24]. With the exception of ultra-heavy neutron stars the APR equation of state allows only modified Urca processes [25–27] which are the dominant microscopic processes that induce bulk viscosity. Direct Urca processes [27, 28] are only possible in the core of a neutron star close to the mass limit which we study in addition. The dominant contribution to the shear viscosity in hadronic matter results from non-Fermi liquid enhanced lepton-lepton scattering [29].

For the strange stars and the quark core of the hybrid stars we use quark matter obeying a simple equation of state in terms of parameters  $c$ ,  $m_s$  and  $B$ ,

$$\begin{aligned} p_{par} &= \frac{1-c}{4\pi^2} (\mu_d^4 + \mu_u^4 + \mu_s^4) - \frac{3m_s^2 \mu_s^2}{4\pi^2} \\ &+ \frac{3m_s^4}{32\pi^2} \left( 3 + 4 \log \left( \frac{2\mu_s}{m_s} \right) \right) - \mathcal{B} + \frac{\mu_e^4}{12\pi^2}. \end{aligned} \quad (10)$$

This is a generalization of the parameterization employed in [30] from which the equilibrium pressure is obtained via the conditions of weak equilibrium  $\mu_s = \mu_d = \mu_u + \mu_e$  and electrical neutrality. The shear viscosity in quark matter arises from non-Fermi-liquid-enhanced quark-quark scattering [31] and the bulk viscosity from non-leptonic flavor-changing weak processes [14, 32]. For our hybrid stars we make the assumption of local electrical neutrality, excluding the possibility of a mixed phase and its wealth of geometric structures.

The equilibrium star configuration is then determined by the general-relativistic Tolman-Oppenheimer-Volkov (TOV) equations [33]. Characteristics of the examples that we consider are given in table I. The susceptibilities  $B$  and  $C$  of the considered forms of matter are given in table II. Finally, the reequilibration parameters  $\Gamma$ ,  $\delta$  and  $\chi$  in the parameterization of the weak rate eq. (1) and the parameters of the shear viscosity eq. (9) are given for the considered forms of dense matter in table III. Note that there are higher non-linearities in the weak rate of hadronic compared to quark matter, which in accordance with eq. (7) yields a steeper rise of the viscosity with amplitude so that suprathreshold effects are even more important in hadronic matter than in quark matter.

	$M [M_\odot]$	$M_{core} [M_\odot]$	$R [km]$	$n_c [n_0]$	$\langle n \rangle [n_0]$	$\Omega_K [kHz]$
NS	1.4	(1.39)	11.5	3.43	1.58	6.02
	2.0	(1.99)	11.0	4.91	2.46	7.68
	2.21	0.85	10.0	7.17	3.37	9.31
SS	1.4	–	11.3	2.62	1.91	6.17
	2.0	–	11.6	4.95	2.43	7.09
HS	1.4	1.06	12.7	2.32	1.17	5.16
	2.0	1.81	12.2	4.89	1.84	6.62

Table I: Properties of the considered models of neutron stars (NS), strange stars (SS) and hybrid stars (HS). We show the mass of the star  $M$ , the mass of the core  $M_{core}$ , the radius  $R$ , the baryon density at the center of the star  $n_c$  given in units of nuclear saturation density  $n_0$ , the average density  $\langle n \rangle$  and the Kepler frequency  $\Omega_K$ . The neutron stars were obtained by solving the relativistic TOV equations for catalyzed neutron matter using the APR equation of state [21] with low density extension [22, 23] and the strange stars with a quark gas bag model with  $c = 0$ ,  $m_s = 150$  MeV and a bag parameter  $B = (138 \text{ MeV})^4$ . Large mass hybrid stars are only found when strong interaction corrections are considered, cf. [30], and we find a  $2 M_\odot$  star for  $c = 0.4$ ,  $m_s = 140$  MeV,  $B = (137 \text{ MeV})^4$ .

### C. R-mode profile

R-modes are normal modes of rotating stars and are obtained from a linear perturbation analysis around the static star configurations discussed above. We consider a star rotating with angular frequency  $\Omega$ . To simplify this analysis it is performed in a Newtonian approximation and in a slow rotation expansion in  $\Omega^2 / (\pi G_N \bar{\rho})$ . The analysis of the damping due to bulk viscosity strictly requires an expansion to next to leading order. The oscillation frequency depends on the frame. For an r-mode with angular dependence  $Y_{m+1}^m$  the frequency in a frame rotating with the unperturbed star  $\omega_r$ , which is relevant for microscopic quantities like the viscosity, and the corresponding frequency  $\omega_i$ , observed by an observer in an inertial frame, are given by

$$\omega_r \equiv \omega = \kappa(\Omega)\Omega \quad , \quad \omega_i = \omega_r - m\Omega \quad (11)$$

where the function  $\kappa$  has an analog expansion and reads to lowest order  $\kappa_0 = 2/(m+1)$ . For dissipation via bulk viscosity the relevant quantity is the density compression due to the r-mode with dimensionless amplitude  $\alpha$ . It vanishes to leading order in the slow rotation expansion and reads at next to leading order [2, 34]

$$\left| \frac{\Delta n}{\bar{n}} \right| \approx \sqrt{\frac{4m}{(m+1)^3(2m+3)}} \frac{2}{(m+1)\kappa(\Omega)} \alpha A R^2 \Omega^2 \cdot \left( \left( \left( \frac{r}{R} \right)^{m+1} + \delta\Phi_0 \right) |Y_{m+1}^m(\theta, \phi)| + \dots \right) \quad (12)$$

where the ellipsis denotes further contributions involving next to leading order corrections of the potentials that are explicitly given in [2]. In this expression  $A$  denotes the inverse squared speed of sound

$$A \equiv \left. \frac{\partial \rho}{\partial p} \right|_0 \quad (13)$$

evaluated at equilibrium. There are different conventions for the amplitude  $\alpha$  in the literature and we follow the convention for the amplitude given in [34] but take into account the corrections to the latter result in [2]. This convention is usually used in the literature [48] and in this case the above expression breaks down for  $\alpha > O(1)$ . For more details on the r-mode expression see Appendix A. In general one must numerically solve a differential equation to obtain  $\delta\Phi_0$ , which is the leading order correction to the gravitational potential, which obeys a differential equation that is given in [4] and generally has to be solved numerically. However, in the special case of a star with a constant density profile  $\delta\Phi_0$  can be shown to be subleading compared to the first term in the inner parentheses of eq. (12). For our numerical analysis below we will make the approximation to neglect the additional second order corrections in the slow rotation expansion given by the ellipsis in eq. (12), which amounts to replacing the Lagrangian perturbation by the Eulerian perturbation, but we include the second order corrections to the frequency eq. (11). General analytic results showed that this is a good approximation for the computation of the small amplitude instability regions [4]. Here we will give semi-analytic results for the saturation amplitudes, valid beyond leading order, that show the influence of the second order terms.

We will see below that, in obtaining a precise assessment of the damping time of large amplitude r-modes, the radial dependence of the density perturbation plays a vital role. The radius enters eq. (12) explicitly and also via the density dependence of the inverse squared speed of sound  $A$  (fig. 1) and the radial density dependence of the star (fig. 2 in [4]). The radial variation of the density is moderate in a strange star, but much more pronounced in neutron stars where the r-mode amplitude grows strongly in the outer regions of the star.

## III. DAMPING TIME SCALES

### A. General expressions

The amplitude of the r-mode oscillations evolves with time dependence  $\exp(i\omega t - t/\tau)$ . We can decompose the decay rate  $1/\tau$  as

$$\frac{1}{\tau(\Omega)} = \frac{1}{\tau_G(\Omega)} + \frac{1}{\tau_B(\Omega)} + \frac{1}{\tau_S(\Omega)} \quad (14)$$

Where  $\tau_G$ ,  $\tau_B$  and  $\tau_S$  are gravitational radiation, bulk viscosity and shear viscosity time scales, respectively.

	$A$	$B$	$C$
hadronic matter	$m_N \left(\frac{\partial p}{\partial n}\right)^{-1}$	$\frac{8S}{n} + \frac{\pi^2}{(4(1-2x)S)^2}$	$4(1-2x)\left(n\frac{\partial S}{\partial n} - \frac{S}{3}\right)$
hadronic gas	$\frac{3m_N^2}{(3\pi^2 n)^{2/3}}$	$\frac{4m_N^2}{3(3\pi^2)^{1/3} n^{4/3}}$	$\frac{(3\pi^2 n)^{2/3}}{6m_N}$
quark matter (gas: $c = 0$ )	$3 + \frac{m_s^2}{(1-c)\mu_q^2}$	$\frac{2\pi^2}{3(1-c)\mu_q^2} \left(1 + \frac{m_s^2}{12(1-c)\mu_q^2}\right)$	$-\frac{m_s^2}{3(1-c)\mu_q}$

Table II: Strong interaction parameters, defined in eqs. (2) and (13), describing the response of the particular form of matter. In the case of interacting hadronic matter a quadratic ansatz in the proton fraction  $x$  parameterized by the symmetry energy  $S$  is employed. The expressions for a hadron and quark gas are given to leading order in  $n/m_N^3$  respectively next to leading order in  $m_s/\mu$ .

Weak process	$\tilde{\Gamma}$ [MeV $^{(3-\delta)}$ ]	$\delta$	$\chi_1$	$\chi_2$	$\chi_3$	Strong/EM process	$\tilde{\eta}$ [MeV $^{(3+\sigma)}$ ]	$\sigma$
quark non-leptonic	$6.59 \times 10^{-12} \left(\frac{\mu_q}{300 \text{ MeV}}\right)^5$	2	$\frac{1}{4\pi^2}$	0	0	quark scattering	$1.98 \times 10^9 \alpha_s^{-5/3} \left(\frac{\mu_q}{300 \text{ MeV}}\right)^{14/3}$	$\frac{5}{3}$
hadronic direct Urca	$5.24 \times 10^{-15} \left(\frac{x n}{n_0}\right)^{1/3}$	4	$\frac{10}{17\pi^2}$	$\frac{1}{17\pi^4}$	0	leptonic scattering	$1.40 \times 10^{12} \left(\frac{x n}{n_0}\right)^{14/9}$	$\frac{5}{3}$
hadronic modified Urca	$4.68 \times 10^{-19} \left(\frac{x n}{n_0}\right)^{1/3}$	6	$\frac{189}{367\pi^2}$	$\frac{21}{367\pi^4}$	$\frac{3}{1835\pi^6}$	nn-scattering	$5.46 \times 10^9 \left(\frac{n}{m_N n_0}\right)^{9/4}$	2

Table III: *Left panel:* Parameters of the general parameterization of the weak rate eq. (1) for different processes of particular forms of matter which determine the damping due to bulk viscosity. The coefficients  $\chi_i$  parameterize the non-linear dependence on the chemical potential fluctuation  $\mu_\Delta$  arising in the suprathreshold regime of the viscosity which is relevant for large amplitude r-modes. *Right panel:* Parameters arising in the parameterization eq. (9) of the shear viscosity for different strong and electromagnetic interaction processes. The leptonic and quark scatterings arise from a non-Fermi liquid enhancement due to unscreened magnetic interactions.

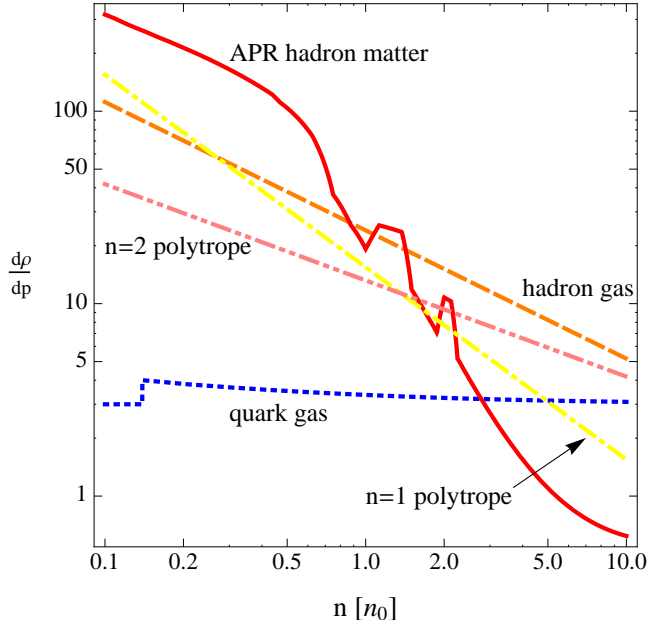


Figure 1: The density dependence of the inverse squared speed of sound  $A \equiv d\epsilon/dp$  (which enters the r-mode profile multiplicatively) for the different forms of matter in table II as well as generic polytropic models. The solid line represents interacting APR matter, the dashed line a hadron gas and the dotted line shows the result for a quark gas. The structure at intermediate densities in the APR curve arises from phase transitions and the use of finite differences to compute the derivative, but due to the mild contribution of the denser inner regions of the star to the damping these have no influence on our results below.

The time scale of the r-mode growth due to gravitational wave emission is given by [34]

$$\frac{1}{\tau_G} = -\frac{32\pi (m-1)^{2m}}{((2m+1)!!)^2} \left(\frac{m+2}{m+1}\right)^{2m+2} \tilde{J}_m G M R^{2m} \Omega^{2m+2} \quad (15)$$

and the damping time due to the shear viscosity can be written as [4]

$$\frac{1}{\tau_S} = \sum_l \frac{(m-1)(2m+1) \tilde{S}_m^{(l)} \Lambda_{\text{QCD}}^{3+\sigma} R}{\tilde{J}_m M T^\sigma} \quad (16)$$

with the radial integral constants

$$\tilde{J}_m \equiv \frac{1}{M R^{2m}} \int_0^R \rho(r) r^{2m+2} dr \quad (17)$$

$$\tilde{S}_m^{(l)} \equiv \frac{1}{R^{2m+1} \Lambda_{\text{QCD}}^{3+\sigma}} \int_{R_i^{(l)}}^{R_o^{(l)}} \tilde{\eta} r^{2m} dr \quad (18)$$

where  $\rho$  is the energy density and  $\Lambda_{\text{QCD}}$  a generic QCD scale introduced to make the constant dimensionless. When several shells with inner radii  $R_i^{(l)}$  and outer radii  $R_o^{(l)}$  and distinct phases and/or transport coefficients are present in a compact star, the damping time integral over the star decomposes into a sum of contributions of the individual shells  $l$ . The bulk viscosity damping time is given by [2]

$$\frac{1}{\tau_B} = \frac{\kappa^2}{\alpha^2 \tilde{J}_m M R^2} \int d^3x \left| \frac{\Delta\rho}{\bar{\rho}} \right|^2 \zeta \left( \left| \frac{\Delta\rho}{\bar{\rho}} \right|^2 \right) \quad (19)$$

Using the general expression for the bulk viscosity eqs. (3) and (5) and expressing the fluctuation in the conserved energy density  $\Delta\rho/\bar{\rho}$  by the same fluctuation of the baryon density  $\Delta n/\bar{n}$ , gives for the damping time the general expression

$$\frac{1}{\tau_B} = \frac{4\pi\Omega^3}{(m+1)^2 \tilde{J}_m M R^2 \kappa} \sum_l \mathcal{T}^{(l)}(a, b). \quad (20)$$

in terms of integrals over the individual shells. Defining the reduced density oscillation

$$\left( \frac{\Delta n}{\bar{n}} \right)_{\text{red.}} \equiv \frac{(m+1)\kappa(\Omega)}{2\alpha\Omega^2} \frac{\Delta n}{\bar{n}} \quad (21)$$

we can write

$$\begin{aligned} \mathcal{T}^{(l)}(a, b) \equiv & \int_{R_i^{(l)}}^{R_o^{(l)}} dr r^2 \int d\theta \sin\theta \left| \left( \frac{\Delta n}{\bar{n}} \right)_{\text{red.}}(r, \theta) \right|^2 \frac{C(r)^2}{B(r)} \\ & \cdot \tilde{\mathcal{I}} \left( aC(r)B(r)^{1/\delta} \tilde{\Gamma}(r)^{1/\delta} \left| \left( \frac{\Delta n}{\bar{n}} \right)_{\text{red.}}(r, \theta) \right|, bB(r)\tilde{\Gamma}(r) \right) \end{aligned} \quad (22)$$

depending on only two independent parameters

$$\begin{aligned} a & \equiv \frac{\kappa_0 \alpha \Omega^2}{\kappa \omega^{1/\delta}} = \frac{2\alpha\Omega^{(2\delta-1)/\delta}}{(m+1)\kappa^{(\delta+1)/\delta}} \\ b & \equiv \frac{T^\delta}{\omega} = \frac{T^\delta}{\kappa\Omega} \end{aligned}$$

Note that in eq. (22) all local quantities can take different values in different shells, as given in tables II and III, but to make the expression readable we do not show the explicit suffixes  $(l)$ . Whereas strange stars are basically homogeneous and consist of a single phase, the crust of neutron and hybrid stars is extremely inhomogeneous and complicated. Although there are no free protons and thereby no Urca processes, the ultra-heavy nuclei present in the inner crust as well as the clusters in potential pasta phases still feature analogous beta-processes. Since oscillations likewise push the system out of beta-equilibrium an analogous suprathreshold enhancement of the bulk viscosity contribution from these phases is expected. However, there are to our knowledge no results for the bulk viscosity in the inner crust, yet [35]. Therefore we will in our numeric results given below neglect the contribution

from the crust and only include the contribution from the core. The core does not have a sharply-defined boundary: we chose it conventionally to be at baryon density  $n_0/4$  corresponding to the lowest point in the APR table, but check the dependence on this choice.

### B. Approximate limits of the bulk viscosity damping time

In the subthermal regime  $\mu_\Delta \ll T$  the bulk viscosity eq. (6) is independent of the r-mode amplitude, so the angular integral in eq. (19) is trivial. The damping time in the subthermal regime is then given by

$$\frac{1}{\tau_B^<} = \frac{16m}{(2m+3)(m+1)^5 \kappa} \frac{R^5 \Omega^3}{\tilde{J}_m M} \sum_l \mathcal{T}_m^{<(l)} \left( \frac{T^\delta}{\kappa\Omega} \right) \quad (23)$$

in terms of the one dimensional radial integral

$$\mathcal{T}_m^{<(l)}(b) \equiv \frac{b}{R^3} \int_{R_i^{(l)}}^{R_o^{(l)}} dr r^2 \frac{A^2 C^2 \tilde{\Gamma}}{1 + \tilde{\Gamma}^2 B^2 b^2} \left( \left( \frac{r}{R} \right)^{m+1} + \delta\Phi_0 \right)^2$$

This expression was used to study the small amplitude instability regions in [4]. Here we want to study the large-amplitude saturation and therefore it is useful to obtain an analytic expression that includes the large-amplitude enhancement of the bulk viscosity. In the intermediate, linear regime and for  $f \ll 1$  the general analytic approximation for the bulk viscosity eq. (7) is valid. Since this local condition has to be fulfilled everywhere in the star, the global parameters  $a$  and  $b$  must be smaller than certain bounds that are determined by the particular properties of the considered stars. We recall from [12] that the approximation is particularly useful for hadronic matter with modified Urca processes where it covers almost the entire range of physical local density amplitudes at millisecond frequencies. A plot of the regions of validity of the individual analytic approximations of the bulk viscosity for different forms of matter is given in [19]. Analogous to the low temperature/high frequency approximation in the subthermal regime eq. (23), in the intermediate, linear regime an explicit evaluation is possible. With the analytic expression for the bulk viscosity eq. (7) the angular integrals over the spherical harmonics arising in the r-mode profile take the form

$$\int d\Omega_{\theta\phi} |Y_{m+1}^m(\theta, \phi)|^{2n} = \frac{4\pi (2n-1)!! (m n)!}{(2(m+1)n+1)!!} \left( \frac{(2m+3)!!}{4\pi m!} \right)^n$$

and this yields a result that apart from the evaluation of the remaining radial integrals is analytic (see also [13, 36])

$$\frac{1}{\tau_{\tilde{B}}} = \frac{16(2m+1)!!\Lambda_{QCD}^{9-\delta}R^5T^\delta\Omega^2}{(m+1)^5(m-1)!\kappa^2\tilde{J}_m\Lambda_{EW}^4M} \sum_{j=0}^N \frac{((2j+1)!)^2(m(j+1))!\chi_j\tilde{V}_{m,j}}{(j+1)!(2(m+1)(j+1)+1)!!} \left( \frac{2m(2m+1)!!}{\pi(m+1)^5m!\kappa^2} \frac{\Lambda_{QCD}^2R^4\alpha^2\Omega^4}{T^2} \right)^j \quad (24)$$

The dependence on all local parameters, like the equation of state, the weak rate, the density dependence of the particular star and its r-mode profile is contained in a few dimensionless radial integral constants ( $\Lambda_{EW}$  is a typical electroweak scale)

$$\tilde{V}_{m,j} \equiv \frac{\Lambda_{EW}^4}{\Lambda_{QCD}^{7-\delta+2(j+1)}R^3} \cdot \int_0^{\mathcal{R}} dr r^2 \tilde{\Gamma}(r) \left( A(r) C(r) \left( \left( \frac{r}{R} \right)^{m+1} + \delta \Phi_0(r) \right) \right)^{2(j+1)} \quad (25)$$

but the dependence on the parameters of the r-mode evolution  $\Omega$ ,  $\alpha$  and  $T$  is entirely explicit in eq. (24). The  $j=0$  term in eq. (24) is precisely the approximate subthermal result eq. (23) in the considered approximation. The constants  $\tilde{V}_j \equiv \tilde{V}_{2,j}$  for the fundamental r-mode are given for several stars in table IV. Although these parameters can vary significantly for different stars, it is quite striking that as far as the bulk viscosity is concerned, the complex details of the individual stars are encoded in a few constants. Note in particular that the parametric form eq. (24) remains valid for the full second order r-mode expression and only the constants eq. (25) are changed. At sufficiently large amplitudes the largest power in the sum in eq. (24) dominates and due to the connection  $\delta = 2N$  the bulk viscosity damping time becomes temperature independent in this approximation. Note also that the integrals  $\tilde{V}_{m,N}$ , as well as the general expression eq. (22) feature an extremely pronounced radial dependence, both due to the explicit radial dependence and the radial dependence of the inverse squared speed of sound  $A$ , that strongly weights the outer parts of the star.

### C. Results for the damping times

Using the expressions for the microscopic parameters given in tables II and III in the general expressions eqs. (15), (16) and (20) we obtain the gravitational and viscosity time scale as a function of their dependent macroscopic parameters. These are given in fig. 2 for the cases of a neutron star with damping due to modified Urca reactions (left panel) and a strange star (right panel) by the solid lines as a function of temperature and for different amplitudes ranging from top to bottom from the subthermal result at infinitesimal amplitude to the extreme case  $\alpha = 10$ .

At sufficiently low temperature the strong increase of the bulk viscosity with the (local) amplitude  $\Delta n/\bar{n}$

damps r-modes with large (global) dimensionless amplitude  $\alpha$  at significantly shorter time scales. As found before from the analytic expression eq. (24), given by the dotted curves, the damping time is temperature independent in this low temperature and intermediate amplitude regime. In contrast, due to the generic form of the bulk viscosity, featuring a universal maximum, the damping of large amplitude r-modes is not enhanced at high temperatures. As a direct consequence of the subthermal maximum of the bulk viscosity [12], the corresponding ‘‘resonant’’ temperature where the damping time is minimal is at roughly  $10^9$  K for strange stars and  $10^{11}$  K for neutron stars. Correspondingly, r-modes are entirely unstable at high temperatures. However, due to the strong suprathreshold enhancement at low temperatures the damping undercuts the gravitational time scale at sufficiently large amplitude so that the r-mode growth will slow down and eventually saturate. The corresponding amplitudes are strikingly very similar for the two different classes of stars, as will be discussed in more detail below. At very large amplitudes  $\alpha \sim O(10)$  the damping times decrease again at all temperatures as a consequence of the behavior of the bulk viscosity [12].

The dot-dashed curves in the neutron star plot on the left panel of fig. 2 show the damping time if the crust is assumed to start already at the higher density  $n_0/2$  instead of  $n_0/4$  so that only the contribution from the correspondingly smaller core is taken into account [49]. Although the damping times are larger, as expected, the amplitude at which the viscous damping can saturate the mode is not drastically changed, so that our results given below remain qualitatively unchanged in this case. Actually, when the damping from the crust would be properly taken into account this should rather enhance the damping and decrease the r-mode amplitude compared to those obtained in this work. In the case of the strange star on the right panel of fig. 2 the dashed curves also show the analytic approximation discussed in appendix B, where the star is assumed to be homogeneous. As can be seen, the corresponding expression eq. (B5) gives an approximate estimate for the damping time at all temperatures and for amplitudes up to the maximum of the viscosity, and only fails at higher amplitudes, where the bulk viscosity cannot saturate the r-mode anymore and where it is thereby not physically relevant. The deviations compared to the numeric result stem mainly from the fact that the density in the strange star is not entirely constant (fig. 2 in [4]).

Previous neutron star analyses [13, 36] have employed an r-mode profile that does not feature the stronger additional radial dependence due to the low density enhance-



star model	shell	$\tilde{J}$	$\tilde{S}$	$\tilde{V}_0$	$\tilde{V}_1$	$\tilde{V}_2$	$\tilde{V}_3$	$\alpha_{sat} (\Omega_K)$
NS $1.4 M_\odot$	core	$1.81 \times 10^{-2}$	$7.68 \times 10^{-5}$	$1.31 \times 10^{-3}$	$4.24 \times 10^{-3}$	$2.02 \times 10^{-2}$	0.105	3.68
NS $1.4 M_\odot$ gas			$4.32 \times 10^{-6}$	$1.28 \times 10^{-4}$	$5.52 \times 10^{-5}$	$3.88 \times 10^{-5}$	$3.03 \times 10^{-5}$	14.3
NS $2.0 M_\odot$		$2.05 \times 10^{-2}$	$2.25 \times 10^{-4}$	$1.16 \times 10^{-3}$	$4.92 \times 10^{-3}$	$3.25 \times 10^{-2}$	0.238	2.52
NS $2.21 M_\odot$	d.U. core	$2.02 \times 10^{-2}$	$5.05 \times 10^{-4}$	$1.16 \times 10^{-8}$	$7.24 \times 10^{-12}$	$5.39 \times 10^{-15}$	—	—
	m.U. core			$9.34 \times 10^{-4}$	$4.42 \times 10^{-3}$	$3.39 \times 10^{-2}$	0.288	2.60
SS eq. (10)	all	$\frac{3}{28\pi}$	$\frac{\hat{\eta}\mu_q^{14/3}}{5\Lambda_{QCD}^{14/3}\alpha_s^{5/3}}$	$\frac{\Lambda_{EW}^4\hat{\Gamma}m_s^4\mu_q^3}{9\Lambda_{QCD}^7(1-c)^2}$	$\frac{\Lambda_{EW}^4\hat{\Gamma}m_s^8\mu_q}{15\Lambda_{QCD}^9(1-c)^4}$	—	—	eq. (28)
SS $1.4 M_\odot$		$3.08 \times 10^{-2}$	$3.49 \times 10^{-6}$	$3.53 \times 10^{-10}$	$1.24 \times 10^{-12}$	—	—	1.16
SS $2.0 M_\odot$		$2.65 \times 10^{-2}$	$4.45 \times 10^{-6}$	$3.58 \times 10^{-10}$	$9.70 \times 10^{-13}$	—	—	1.56
HS $1.4 M_\odot$		quark core	$1.70 \times 10^{-2}$	$3.11 \times 10^{-6}$	$1.38 \times 10^{-10}$	$1.75 \times 10^{-13}$	—	—
	hadr. core	$9.71 \times 10^{-7}$		$1.39 \times 10^{-3}$	$4.70 \times 10^{-3}$	$2.23 \times 10^{-2}$	0.116	3.66
HS $2.0 M_\odot$	quark core	$2.00 \times 10^{-2}$	$5.25 \times 10^{-6}$	$3.76 \times 10^{-10}$	$7.75 \times 10^{-13}$	—	—	1.59
	hadr. core		$5.24 \times 10^{-6}$	$1.07 \times 10^{-3}$	$4.12 \times 10^{-3}$	$2.31 \times 10^{-2}$	0.134	2.94

Table IV: Radial integral parameters and static saturation amplitude of a  $m=2$  r-mode for the stars considered in this work. The constant  $\tilde{J}$ ,  $\tilde{S}$  and  $\tilde{V}_i$  are given by eqs. (17), (18) and (25), respectively, using the generic normalization scales  $\Lambda_{QCD} = 1$  GeV and  $\Lambda_{EW} = 100$  GeV. Note that the subthermal parameter  $\tilde{V}_0$  corresponds to  $\tilde{V}$  in [4] where the subscript was omitted for simplicity and the strange star expressions are given to leading order in  $m_s/\mu$ .

ment of the inverse squared speed of sound  $A$ , shown in fig. 1, for a realistic equation of state. E.g. the r-mode profile given in eq. (6.6) of [37] features roughly a generic  $r^3$ -dependence. The strong r-dependence in our present treatment, however, strongly amplifies the damping in the outer regions of the star. Therefore, the contribution of the crust to the viscous damping should be relevant and would further decrease the saturation amplitude. The current restriction of our analysis to the core presents therefore an upper bound for the saturation amplitude obtained when the damping of the whole star is considered. The second order effects in contrast increase the small amplitude instability region [2] and can correspondingly be expected to likewise increase the saturation amplitude. A more thorough treatment of all these effects in the future is clearly desirable.

#### IV. SATURATION AMPLITUDES

Because of the strong decrease of the viscous damping time due to the suprathreshold enhancement the damping can dominate at sufficiently large amplitudes. In this case the definition of the instability regions have to be extended. The latter are standardly defined in the subthermal regime and are independent of the amplitude. One could extend this concept by the definition of amplitude dependent instability regions which would shrink with increasing amplitude. However, since the amplitude can neither be inferred from observation nor is it a parameter that can be dialed, but is rather determined dynamically, we refrain from this possibility and rather introduce the concept of a *static saturation amplitude*. The latter is defined by the amplitude at which the r-mode would saturate at fixed temperature and frequency and is given by the solution of the equation

$$\frac{1}{\tau_G(\Omega)} + \sum_l \left( \frac{1}{\tau_S^{(l)}(T)} + \frac{1}{\tau_B^{(l)}(T, \Omega, \alpha_{sat})} \right) = 0 \quad (26)$$

where  $l$  runs over the contributions from the different shells of the star. The boundaries of the above mentioned amplitude dependent instability regions are by definition simply the contour lines  $\alpha_{sat}(T, \Omega) = \text{const.}$  and the boundary of the classic instability region, in particular, corresponds to  $\alpha_{sat} = 0$ . In case several solutions of eq. (26) exist, only the smallest one is physical and if no solution exists then viscous damping alone cannot saturate the r-mode according to this definition. Actually, at the same time the r-mode grows, the star generally also cools or reheats and spins down respectively up so that the above amplitudes do not have to be reached. In particular the star could leave the parameter regions where a saturation according to the above criterion is not possible before the r-mode can actually explode.

##### A. Analytic approximation

Similar to the analytic expression for the boundary of the instability region [4] an analytic expression for the static saturation amplitude can be obtained. The analytic linear approximation  $\tau_B^{\sim}$  applies as long as the r-mode amplitude is small enough so that the bulk viscosity is sufficiently below its maximum. When the r-mode amplitude is at the same time large enough that the highest power in eq. (24) dominates, the damping time becomes temperature independent. Both conditions are met sufficiently far inside the instability region so that the damping time simplifies to

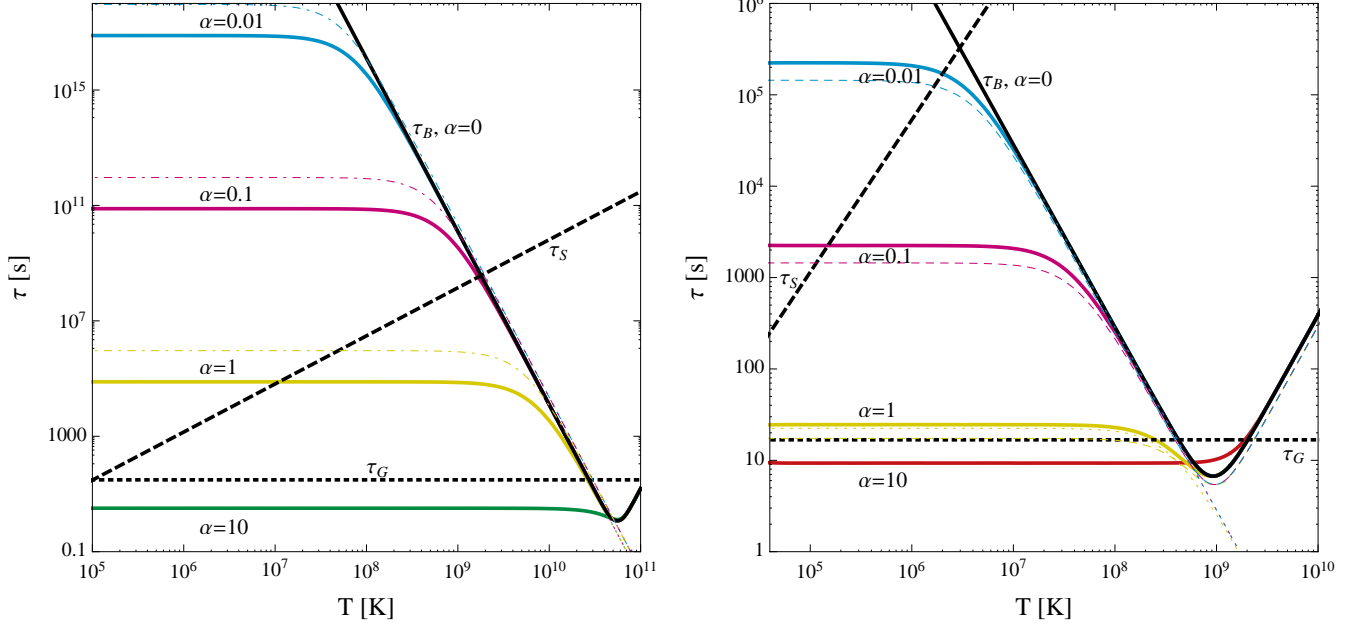


Figure 2: The relevant r-mode time scales for  $1.4 M_{\odot}$  stars rotating at their Kepler frequency. *Left panel:* Neutron star. *Right panel:* Strange star. The dotted horizontal line presents the time scale  $\tau_G$  associated to the growth of the mode due to gravitational wave emission. The dashed rising curve shows the damping time  $\tau_S$  due to shear viscosity. The damping time  $\tau_B$  due to bulk viscosity is given for different dimensionless r-mode amplitudes  $\alpha = 0, 0.01, 0.1, 1$  and  $10$  by the solid curves. The thin dotted curves correspond to the analytic linear approximation eq. (24) and are below the shown plot range for the largest amplitude. The thin dot-dashed curves on the left panel show the change when only a smaller core (ranging to a density of  $n_0/2$  instead of  $n_0/4$ ) is taken into account. The thin dashed curves on the right panel represent the approximate analytic expression eq. (B5) given in the appendix which is not valid above the maximum of the bulk viscosity and therefore not shown for the large amplitude results.

$$\frac{1}{\tau_B} \xrightarrow{j=N=\delta/2} \frac{2^{4+N} m^N ((2m+1)!!)^{N+1} ((2N+1)!!)^2 (m(N+1))! \chi_N \tilde{V}_{m,N}}{\pi^N (m+1)^{5(N+1)} (m!)^N (m-1)! (N+1)! (2(m+1)(N+1)+1)!! \kappa^{2N+2} \tilde{J}_m} \frac{\Lambda_{\text{QCD}}^9 R^{5+4N} \alpha^{2N} \Omega^{4N+2}}{\Lambda_{\text{EW}}^4 M}$$

At saturation this has to match the gravitational time scale  $1/\tau_B + 1/\tau_G = 0$  which yields the general result

$$\alpha_{\text{sat}} = \left( \frac{\pi^{1+\delta/2} (m-1)^{2m} (m+1)^{3+5\delta/2-2m} (m+2)^{2+2m} ((m-1)!)^{1+\delta/2} (\frac{\delta}{2}+1)! (2(m+1)(\frac{\delta}{2}+1)+1)!! \kappa^{\delta+2}}{2^{\delta/2-1} ((2m+1)!!)^{3+\frac{\delta}{2}} ((\delta+1)!!)^2 (m(\frac{\delta}{2}+1))! \chi_{\frac{\delta}{2}}} \right)^{1/\delta} \cdot \frac{\tilde{J}_m^{2/\delta} \Lambda_{\text{EW}}^{4/\delta} G^{1/\delta} M^{2/\delta}}{\tilde{V}_{m,\frac{\delta}{2}}^{-1/\delta} \Lambda_{\text{QCD}}^{9/\delta} R^{2+(5-2m)/\delta} \Omega^{2-2m/\delta}} \quad (27)$$

where  $\kappa$  is defined by eq. (11). In the cases of strange stars with non-leptonic processes  $\delta = 2$  and hadronic matter with modified Urca processes  $\delta = 6$  this gives for the  $m = 2$  r-mode

$$\alpha_{\text{sat}}^{(SS)} \approx 5.56 \cdot 10^{-5} \frac{\tilde{J}}{\tilde{V}_1^{1/2}} \frac{M_{1.4}}{R_{10}^{5/2}} \approx 1.61 \frac{(1-c)^2 M_{1.4}}{m_{150}^4 \mu_{300}^{1/2} R_{10}^{5/2}} \quad (28)$$

$$\alpha_{\text{sat}}^{(NS)} \approx 10.8 \frac{\tilde{J}^{1/3}}{\tilde{V}_3^{-1/6}} \frac{M_{1.4}^{1/3}}{R_{10}^{13/6} \Omega_{ms}^{4/3}}$$

where  $\tilde{J} \equiv \tilde{J}_2$  and  $\tilde{V}_i \equiv \tilde{V}_{2,i}$  are given for the normalization scales used in table IV. Here  $m_{150}$ ,  $\mu_{300}$ ,  $M_{1.4}$ ,  $R_{10}$  and  $\Omega_{m_s}$  are the effective strange quark mass in units of 150 MeV, the quark chemical potential in units of 300 MeV, the stars mass in units of  $1.4 M_\odot$ , the radius in units of 10 km and the angular velocity in units of  $2\pi$  kHz corresponding to a millisecond pulsar, respectively. For strange stars the above expression for the intermediate amplitude bulk viscosity damping time has the same frequency dependence as the gravitational time scale eq. (15), so  $\alpha_{sat}$  is basically constant throughout the instability region. However, it rises with decreasing frequency for neutron stars where the frequency dependence of the bulk viscosity is weaker. In contrast to the analytic expressions for the extrema of the instability region given in [4], which are very insensitive to the microscopic transport parameters, the saturation amplitude is more sensitive to the suprathermal bulk viscosity parameter  $\tilde{V}$ . Whereas the saturation amplitude of neutron stars still depends on  $\tilde{V}$  rather mildly due to the power 1/6, the saturation amplitude for strange stars obtained from the generic equation of state eq. (10) decreases with the “interaction parameter”  $c$  and even more strongly with the effective strange quark mass  $m_s$ .

## B. Numeric solution

Let us now discuss the numerical solution for the saturation amplitude. In the following plots figs. 3 to 7 the static saturation amplitude is shown as a function of temperature and amplitude and they feature generally 3 distinct regions. The light (blue) surface shows the saturation amplitude where the r-mode growth is stopped by suprathermal damping. Due to the characteristic behavior of the bulk viscosity [12] which does not feature an amplitude enhancement for temperatures above the temperature  $T_{max}$  eq. (4), the r-mode is not damped at all by viscous effects in the high temperature regime as denoted by the dark (red) area on the right hand side. In the flat (green) region surrounding the instability region the r-mode is entirely stable and already damped by the shear or the subthermal bulk viscosity so that  $\alpha_{sat} = 0$ .

The left panel of fig. 3 shows the static saturation amplitude for the  $m = 2$  r-mode of a  $1.4 M_\odot$  neutron star. Although this might be hard to see in certain regions of the plot, the saturation amplitude rises steeply, within a narrow interval, from zero at the boundary of the instability region towards its interior. At large frequencies it reaches a plateau value that is nearly independent of the temperature as predicted by the analytic expression eq. (27). As described by the latter expression, inside the instability region the saturation amplitude rises strongly with decreasing frequency and since the instability region shrinks in width and eventually ends at low frequencies where the amplitude vanishes and the mode is damped, it features a peak-like structure. The maximum static saturation amplitude reached at the peak is in this

case unphysically large whereas the plateau value at the Kepler frequency is still roughly 3.5. The suprathermal bulk viscosity can therefore in principle saturate r-modes within the lower part of the instability region. However, in the present case, where only the damping of the core is taken into account, the static saturation amplitudes are at the limit where a standard r-mode analysis is valid. Moreover these amplitudes are so far larger than those of alternative saturation mechanisms [7–10]. It is interesting to mention once more, though, that the extreme radial dependence of the r-mode profile eq. (12) strongly weights the outer regions of the star due to power law dependences of the inverse bulk viscosity damping time eq. (19) with exponents  $O(30)$  for neutron and hybrid stars which is further enhanced by the density dependence of the inverse speed of sound. The contribution of the crust could thereby be decisive to obtain a realistic estimate of the impact of the non-linear viscosity. In this context it is also important that a similar enhancement of the bulk viscosity has been found for superfluid matter [38]. As noted in [4] there is a second instability region at high temperatures above  $10^{11}$  K and as argued above the suprathermal bulk viscosity cannot saturate the r-mode in this high temperature regime. It is an interesting question if the r-mode can become large during this initial part of a star’s evolution, and if so whether the r-mode is saturated at sufficiently small values by other non-linear mechanism or if the r-mode growth is not stopped before it reaches the regime where the structural stability of the star is at stake. In the latter case this instability phase might extend the violent supernova stage and actively shape the remnant by additional mass shedding and thereby determine its initial size and angular momentum. We will discuss these points further in the conclusion.

The saturation amplitude for the  $1.4 M_\odot$  strange star is shown on the left panel of fig. 4. Since the maximum of the stability window is above the Kepler frequency there are in this plot two separate parts of the instability region. As predicted by eq. (27) the plateau value of the saturation amplitude in the lower part is approximately temperature and frequency independent. Strikingly it is of similar size as the saturation amplitude for the  $1.4 M_\odot$  neutron star at its Kepler frequency. The high temperature part of the instability region where the viscosity again cannot saturate the r-mode extends in this case down to lower temperatures than for neutron stars.

The left panel of fig. 5 shows the corresponding plot for the  $1.4 M_\odot$  hybrid star. As found previously in [4] the instability region has here three parts that are separated by two stability windows arising from the resonant behavior of the bulk viscosities in the different shells. Due to their parametrically different temperature dependence the bulk viscosity of the quark shell dominates at low temperature, whereas the bulk viscosity of the hadronic shell dominates at high temperatures. Correspondingly the saturation amplitude in the low temperature part of the instability region shows the qualitative behavior

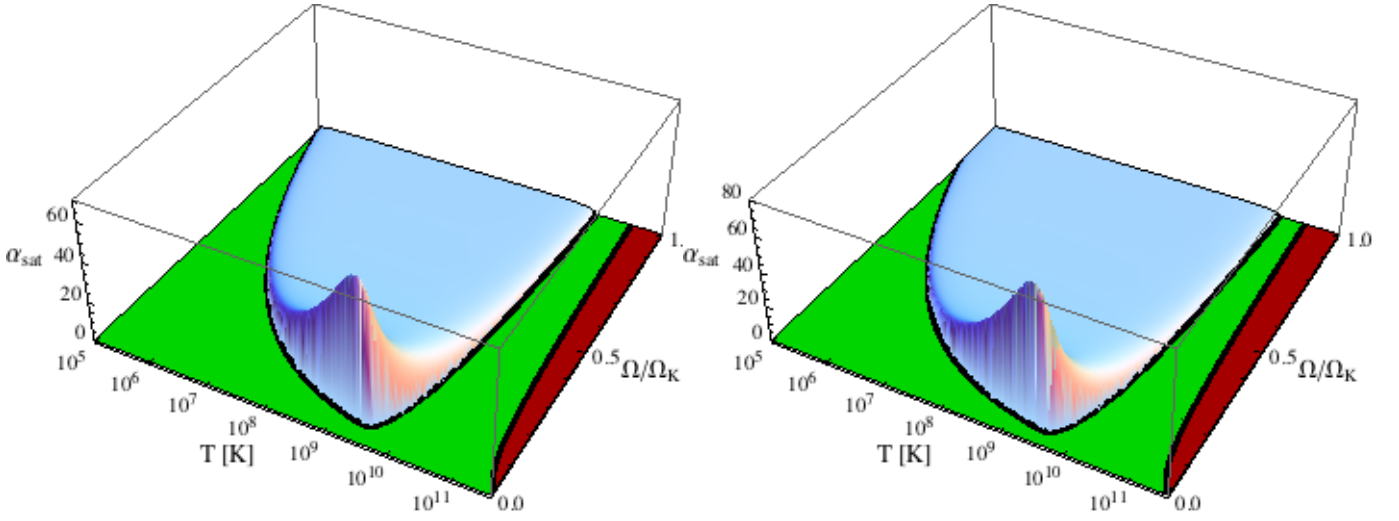


Figure 3: The static saturation amplitude, at which the r-mode growth is stopped by suprathreshold viscous damping for the APR neutron stars. *Left panel:*  $1.4 M_{\odot}$ . *Right panel:*  $2.0 M_{\odot}$ . The light (green) shaded area denotes the stable region where the r-mode is damped away. At large frequencies a plateau with amplitudes  $O(1)$  is reached. In the dark (red) region at high temperatures the r-mode is entirely unstable and cannot be saturated by viscous effects.

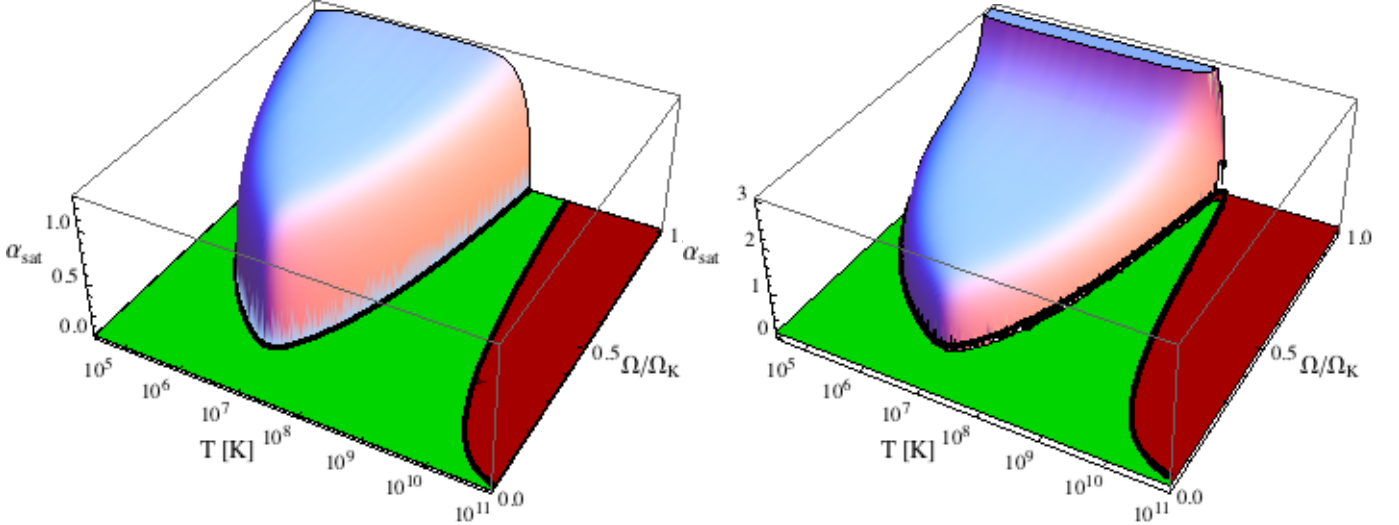


Figure 4: The saturation amplitude for the considered strange stars. *Left panel:*  $1.4 M_{\odot}$ . *Right panel:*  $2.0 M_{\odot}$ . In the latter case the suprathreshold viscosity cannot stop the r-mode instability at frequencies larger than the maximum frequency of the stability window (where the saturation amplitude diverges) - for the considered star slightly below the Kepler frequency - as well as in the high temperature part of the instability region. The saturation amplitudes of the plateau in the lower part of the instability region are of the same order as in the hadronic case shown in fig. 3.

found for strange matter whereas the intermediate temperature part shows the qualitative behavior found for hadronic matter. Since the region where the peak in fig. 3 is located is “cut out” by the stability window, the remaining peak of the hadronic intermediate part of the instability region in fig. 5 reaches only a much lower amplitude.

The result for the heavy  $2.0 M_{\odot}$  neutron star is given on the right panel of fig. 3. As had been found previously in [4] the instability region is larger for such heavy stars. The figure shows in addition that saturation occurs at a

somewhat higher amplitude. The  $2.0 M_{\odot}$  strange star is given on the right panel of fig. 4. In this case the maximum of the stability window is below the Kepler frequency. Similar to the high temperature behavior discussed before, the r-mode cannot be damped by viscous effects above this maximum. It is interesting to recall from [4] that in the case of quark matter an approximate analytic expression for the location of the maximum of the stability window exists

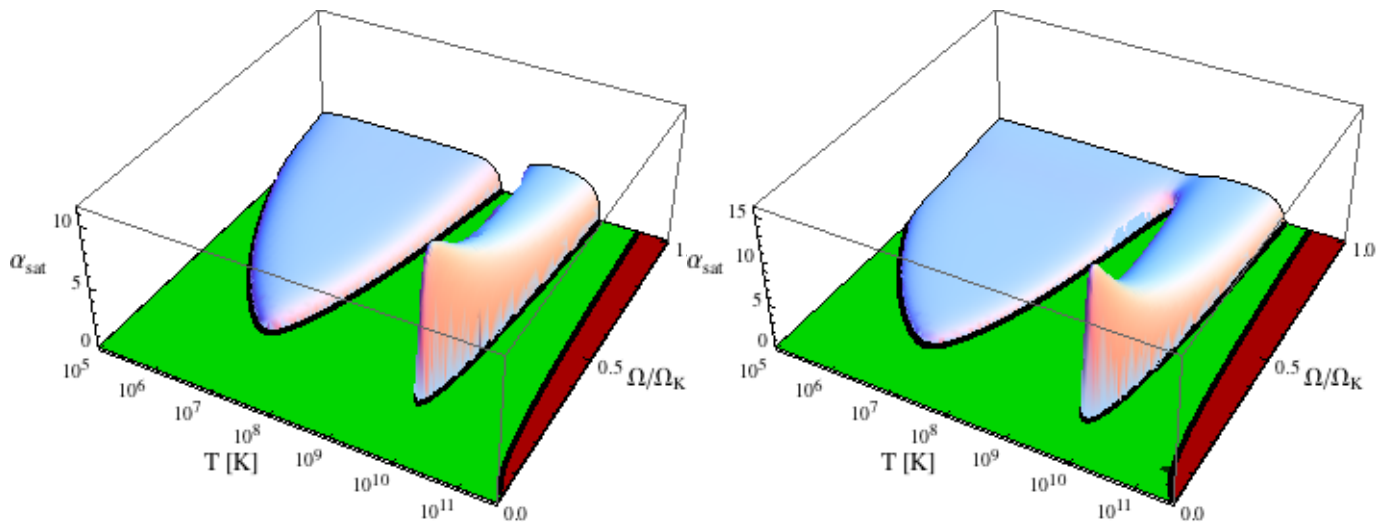


Figure 5: The saturation amplitude for the considered hybrid stars. *Left panel:*  $1.4 M_{\odot}$ . *Right panel:*  $2.0 M_{\odot}$ . The saturation in the low temperature part of the instability region is mostly established by the bulk viscosity of the quark core, whereas the saturation in the mid temperature part comes mainly from the hadronic shell.

$$\Omega_{max}^{(SS)} \approx \frac{0.434 m_s^{4/3} R^{1/3}}{(1-c)^{1/3} G^{1/3} M^{2/3}} \quad (29)$$

$$T_{max}^{(SS)} \approx \frac{0.210 (1-c)^{1/3} m_s^{2/3} R^{1/6}}{\hat{\Gamma}^{1/2} G^{1/6} \mu_q^{3/2} M^{1/3}} \quad (30)$$

where  $\hat{\Gamma} \equiv \tilde{\Gamma}/\mu_q^5$ . This shows that in addition to a large star mass, a small effective strange quark mass in the quark matter equation of state eq. (10) increases the total instability region both at high frequency and high temperature. In contrast, for the heavy  $2.0 M_{\odot}$  hybrid star shown on the right panel of fig. 5 such a total instability region does not arise since although the quark core cannot saturate the r-mode, the hadronic shell alone still provides sufficient damping to do so. In summary r-modes in massive stars are more unstable than in light stars since both their small amplitude instability regions are larger and they are less efficiently saturated by the large amplitude enhancement of the bulk viscosity.

The left panel of fig. 6 shows the static saturation amplitude for a neutron star with  $2.21 M_{\odot}$  which is the maximum mass allowed by the APR equation of state. In this case direct Urca reactions are possible in a small inner core region of mass  $0.85 M_{\odot}$ . As had already been observed in [4], direct Urca reactions only slightly alter the instability boundary by a small notch at its right hand side. Since suprathreshold damping from outer layers dominates due to the strong radial dependence of the r-mode the static saturation amplitude is likewise only slightly reduced by the small direct Urca core. However, because the size of the inner direct Urca core depends strongly on the equation of state and there are equations of state where the direct Urca core is considerably larger, we show on the right panel of fig. 6 for comparison the (unphys-

ical) case that the direct Urca reactions are artificially switched on in the entire core. This represents an upper limit for the possible effect of direct Urca reactions and shows that in this extreme case the static saturation amplitude at large frequency is reduced and the increase towards lower frequencies is considerably weakened according to the  $1/\Omega$ -behavior predicted by eq. (27).

In contrast to the previous results that evaluated the damping time eq. (19) numerically the top, left panel of fig. 7 employs the approximate analytic expression eq. (24) for the  $m = 2$  mode of the  $1.4 M_{\odot}$  neutron star. Comparing it to the numerical result in fig. 3 shows that the corrections are very small and because the maximum of the bulk viscosity of hadronic matter with modified Urca reactions is reached only for large amplitudes, eq. (24) provides a very good approximation in this case. In contrast, the use of the linear approximation which neglects the large amplitude decrease of the bulk viscosity, strongly overestimates the damping for the case of strange stars and misses the previously discussed total instability region at high frequency in fig. 4.

Fig. 7 also shows the saturation amplitudes of different multipole r-modes, given for the first four multipoles  $m = 2$  to 5 of the  $1.4 M_{\odot}$  neutron star. The higher multipoles saturate at lower amplitudes than the  $m = 2$  and therefore the use of the linear approximate is well justified in this case. Interestingly, although the right segments of the lower part of the instability boundary of these higher order r-modes had recently been shown to be very similar to that of the fundamental  $m = 2$  mode [4], fig. 7 shows that the saturation amplitude of these modes decreases dramatically by roughly an order of magnitude with increasing multipole order. Therefore, these higher multipoles should not be very important for the spin-down evolution since the spin-down torque due to gravitational wave emission depends strongly on the

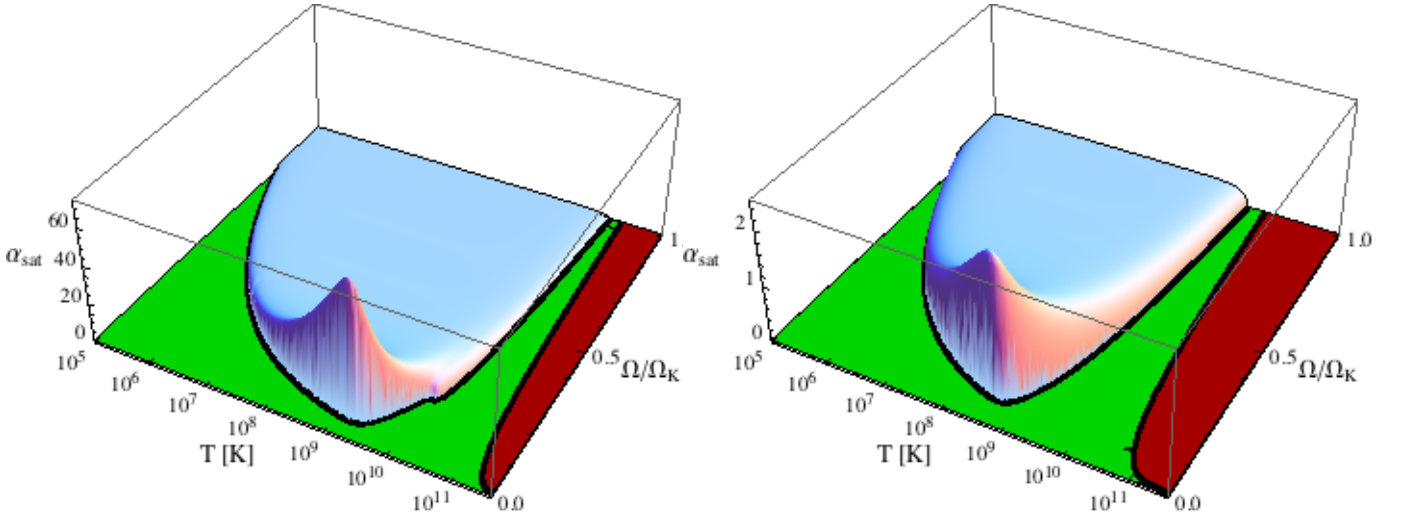


Figure 6: The static saturation amplitude, at which the r-mode growth is stopped by suprathermal viscous damping for the APR neutron stars at the maximum mass  $2.21 M_{\odot}$ , where direct Urca processes become allowed. *Left panel:* direct Urca is only allowed in a small inner core region, see Table I. *Right panel:* the same model when direct Urca is artificially turned on in the entire core.

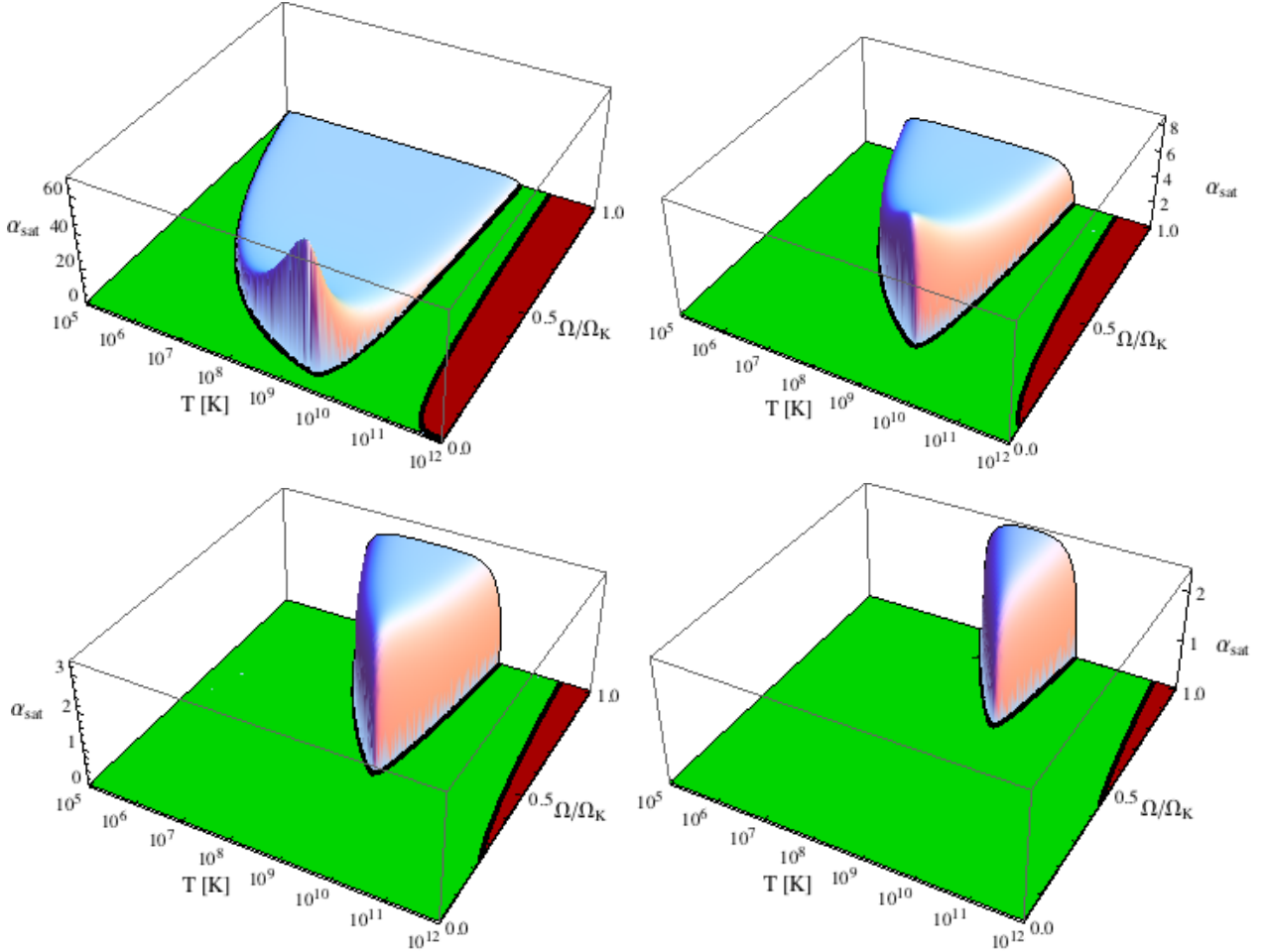


Figure 7: Saturation amplitudes for the first four multipole r-modes of the  $1.4 M_{\odot}$  neutron star (top, left:  $m = 2$ ; top, right:  $m = 3$ ; bottom, left:  $m = 4$ ; bottom right:  $m = 5$ ). The results are obtained in the linear approximation eq. (24). Note the different orders of magnitude of the saturation amplitudes which decrease steeply for higher r-modes.

amplitude [5]; for sufficiently small amplitude modes this dependence is quadratic. So if the suprathreshold damping is responsible for the r-mode saturation, the restriction to the lowest order mode, that had been employed in all present analyses, should be a very good approximation.

The saturation amplitudes of the different  $1.4 M_{\odot}$  stars are finally compared with each other and the analytic approximation eq.(24) in fig.8. Surprisingly, all stars feature saturation amplitudes of the same order of magnitude for millisecond pulsars, despite their very different microscopic and structural aspects. As noted before, for larger oscillation periods hadronic stars and to some extent also hybrid stars feature considerably larger saturation amplitudes than strange stars due to the parametrically different frequency dependence, see eq.(27). The analytic approximation yields in most cases a reasonable approximation to the full results with errors below the 10% level. In general the analytic result overestimates the actual amplitude since it only describes the result far away from the boundaries and boundary effects play a role. In contrast for the strange star the analytic approximation strongly underestimates the saturation amplitude since the considered frequency is in this case close to the critical frequency, where the saturation amplitude diverges, see fig. (4). Yet, even in such extreme cases the analytic approximation provides an important and reliable estimate for the order of magnitude of the static saturation amplitude which, as will be discussed in more detail below, provides an upper limit for saturation amplitudes taken in dynamical star evolutions.

## V. CONCLUSIONS

Using the recent general results for the bulk viscosity that include its non-linear behavior at large amplitudes we have derived expressions for the r-mode damping time that show that in the regime below the resonant temperature of the bulk viscosity, large amplitude r-modes are damped on considerably shorter time scales than low amplitude oscillations. In contrast, the universal maximum of the bulk viscosity found in [12] implies that at very high temperatures and frequencies r-modes cannot be damped at all by viscous effects since there is no enhancement in the suprathreshold limit. We find that for most stars considered in this work the corresponding critical frequency is above the Kepler frequency. On the other hand the r-modes of all considered stars are unstable at temperatures that are expected to be present when a proto-neutron star is created. At lower temperatures our results lead to an extension of the concept of the instability region of an r-mode since the latter is only initially unstable at small amplitudes but the suprathreshold viscous damping can saturate the r-mode growth at finite amplitudes. We find that well within the instability region the static saturation amplitude  $\alpha_{sat}$  defined in the text is temperature independent and takes values  $O(1)$  at milli-second frequencies for all considered

stars. This is incidentally the order of magnitude that had been assumed in early r-mode analyses [5]. Yet, the static values obtained here represent only an upper limit for the actual amplitude reached in the dynamic evolution. Our numeric results are confirmed by approximate analytic expressions which reveal the dependence of these results on the various underlying parameters. We also studied higher multipoles and find that although the first few multipoles have instability regions that are sizable, they feature significantly lower saturation amplitudes and should thereby be far less relevant for the star evolution compared to the fundamental  $m=2$  mode.

It is interesting to compare our saturation mechanism and the obtained results for the saturation amplitudes with previously proposed mechanisms. In general when there are different competing saturation mechanisms, the one with the smallest saturation amplitude should dominate and effectively saturate the mode. Explicit numerical analyses of the general relativistic hydrodynamical equations [6, 9, 10] would present the ideal way to study the saturation and star evolution. Whereas some of these studies find saturation only at large amplitudes, in others the r-mode can be completely destroyed by the decay into daughter modes once it exceeds amplitudes  $O(10^{-2})$  [10], see also [39]. However, the numerical complexity limits these analyses so far to unphysically large values of the radiation reaction force that are orders of magnitude above the physical value and it is not clear to what extent the obtained results can be extrapolated to the physical case. Another proposed saturation mechanism relies on the non-linear coupling of different oscillation modes [7, 8, 39, 40]. These analyses find that this mechanism could saturate r-modes at amplitudes as low as  $O(10^{-5})$ . Due to the considerable difficulties of a complete description of such a mode coupling mechanism, these analyses have to rely on model systems of generic coupled oscillators without a detailed connection to the complicated coupling of collective star oscillations. In summary, within the present approximation to neglect the neutron star crust, competing mechanisms will very likely dominate and saturate the r-mode at lower values than the suprathreshold enhancement of the viscosity. However, these mechanisms still involve simplifications and uncertainties. Our novel saturation mechanism, in contrast, relies on standard viscous effects and microscopic physics that is quantitatively well understood.

Let us now discuss the implications of our results for the spin-down of compact stars. In the supernova formation process where a much larger star contracts to a very compact object that takes over the angular momentum it seems plausible that fast rotating proto-neutron stars could be formed which spin with frequencies close to the Kepler limit. According to our results r-mode oscillations are unstable in this initial hot stage  $T \gtrsim 10^{10} K$  and cannot be saturated by viscous effects for all considered forms of dense matter. Generically, the cooling is very fast in this regime so that the evolution could leave this instability region before large amplitude r-modes de-



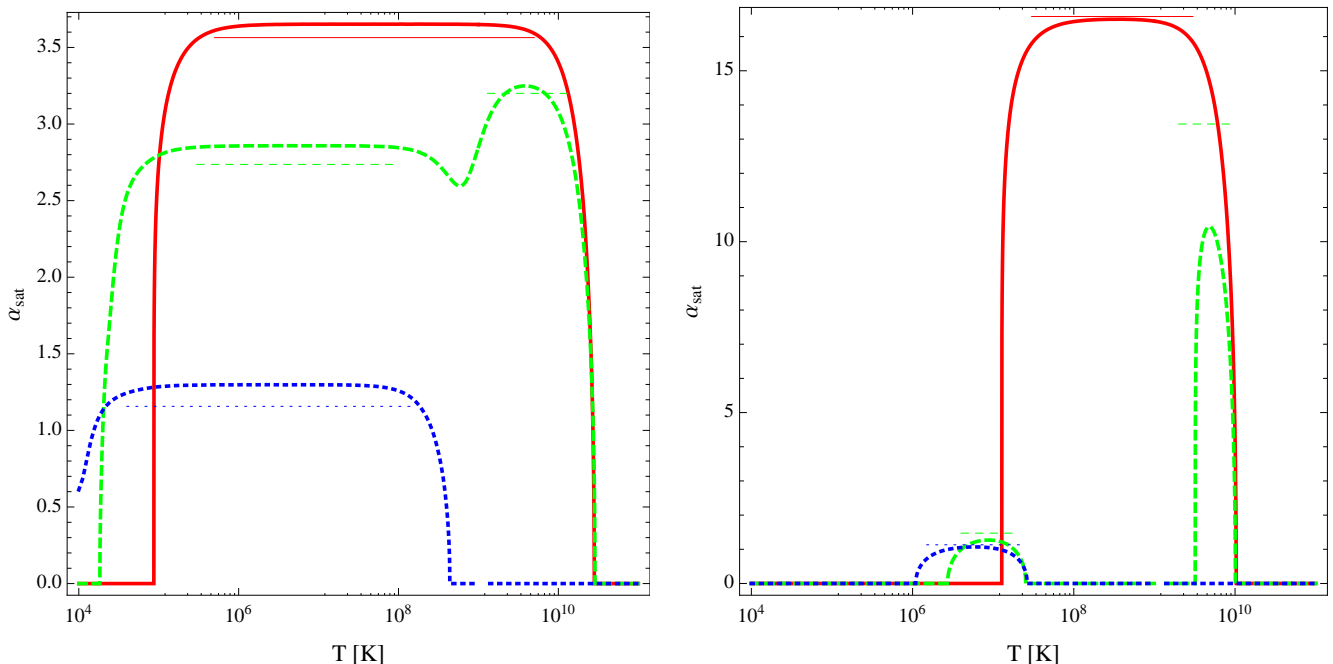


Figure 8: Comparison of the saturation amplitudes for the different  $1.4 M_{\odot}$  stars. *Left panel:* Stars spinning with a period of 1 ms. *Right panel:* Same for stars rotating with a period of 4 ms. Shown are the considered neutron star (solid), the hybrid star (dashed) and the strange star (dotted). The thick curves present the numerical results and the thin horizontal segments denote the analytic values obtained from eq. (27).

velop or spin down the star. The star will then cool until it reaches the lower instability zone and the r-mode develops. According to fig. 8 in this regime the r-mode can be saturated by viscous damping. For strange stars such a saturation does not seem to be required at all since the instability region is in this case located at comparably low temperatures [41] where the cooling becomes slow and the star either quickly spins down [42], or when reheating effects are considered it reheats again [43], and leaves the instability region before the amplitude becomes large. In this case the evolution wiggles around the instability line thereby spinning down the star, but this can take billions of years due to the strong reheating.

In contrast in the case of neutron and hybrid stars without strangeness, the instability region is reached at large temperatures where cooling is still fast and reheating effects are moderate, so that the evolution quickly penetrates the instability region and a saturation mechanism is indeed required to stop the r-mode growth [5]. Since the static saturation amplitude increases continuously at the boundary of the instability region the discussed *static* value does not have to be reached but a *dynamic* equilibrium could be established at a lower saturation amplitude that is reached once the r-mode is sufficiently large that the spindown becomes efficient. Due to this the viscous saturation could dominate competing saturation mechanisms. Once the r-mode is saturated, the question is which one of two competing processes, cooling or spin-down, is faster. Since the cooling is slow-

ing down at lower temperatures it is likely that the spindown wins and the evolution leaves the instability region near its lower boundary. In this case no young compact stars with frequencies larger than a tenth of the Kepler frequency would be possible which is in good agreement with observations. An answer to the above questions requires a detailed study of the combined spin-down and cooling evolution of the star which will be presented elsewhere.

Strikingly our results suggest even another possibility for the spindown of young stars that would be even faster and more violent. The core bounce during the supernova process should excite rather large amplitude oscillation modes in the forming compact core. Since r-modes are unstable in this regime [4] these will grow further. Because of the initial high temperatures, neutrinos are trapped inside the proto-neutron stars for roughly a minute [44]. Since a neutron star crust, that could provide an efficient damping mechanism [11], is not formed at this point and as our results show viscous effects cannot stop the r-mode growth, the amplitude could indeed become large if other non-linear saturation mechanisms likewise cannot operate efficiently in this turbulent environment. In this case the loss of angular momentum could proceed not by gravitational wave emission but by actual mass shedding and thereby effectively as an extension of the supernova explosion that is driven by r-modes. Since such a violent spindown should be fast the star could end up at the lower boundary of the high



temperature instability region before the star becomes transparent to neutrinos and the cooling process starts. Clearly, in this initial stage, which cannot rigorously be separated from the aftermath of the supernova explosion, the dynamics is highly non-linear and our simple r-mode analysis might not directly apply. Whether such a mechanism is feasible will therefore require further study, but this mechanism would naturally explain the observed absence of fast, young pulsars independent of their internal composition and it is striking that the frequencies of the high temperature instability boundary also seem to agree well with fastest pulsars that are young enough that they cannot be spun up by accretion [45].

Finally, r-modes should also be relevant for old accreting stars in binary systems that are spun up and could enter the instability region at low temperatures from below [46]. As discussed in [4], strange and hybrid stars feature stability windows at low temperatures where the r-mode is absent, so that such stars could accelerate to frequencies close to the Kepler frequency. In contrast for neutron stars there is no stability window at low temperatures so that an accreting star would enter the unstable regime already at low frequencies. Recall that the saturation amplitude of neutron stars due to bulk viscosity has a characteristic form with a pronounced peak close to the minimum of the instability region. In case the r-mode is saturated by suprathreshold bulk viscosity, the steep rise of the amplitude close to the maximum should spin down the star quickly and so that it cannot penetrate deep into the instability region. This means that such stars should cluster close to the boundary which might be a signature once more observational data for the temperature of compact stars becomes available.

### Acknowledgments

We thank Nils Andersson, Greg Comer, Brynmor Haskell, Prashant Jaikumar, Andreas Reisenegger, Andrew Steiner and Ira Wasserman for helpful discussions. This research was supported in part by the Offices of Nuclear Physics and High Energy Physics of the U.S. Department of Energy under contracts #DE-FG02-91ER40628, #DE-FG02-05ER41375.

### Appendix A: R-mode and amplitude conventions

In this appendix we review a few standard expressions for r-modes and discuss different conventions used in the literature. The form of the r-mode oscillation is most conveniently derived [47] from the underlying equations that determine the fluctuation of the potential  $\delta U = \delta h + \delta \Phi$ , where  $h$  is the enthalpy and  $\Phi$  the gravitational potential, since then the hydrodynamic Euler equation for the harmonic, cylindrically symmetric perturbation reduces from a differential to an ordinary linear equation and can be solved analytically by matrix inversion. The ex-

pression for  $\delta U$  reads to leading order in a slow rotation expansion

$$\delta U \approx \sqrt{\frac{m}{\pi(m+1)^3(2m+1)!}} \alpha R^2 \Omega^2 \left(\frac{r}{R}\right)^{m+1} P_{m+1}^m(\mu) e^{im\phi} \quad (\text{A1})$$

The velocity fluctuation is obtained from  $\delta U$  by application of a differential operator [47] and yields to leading order in a slow rotation expansion [34]

$$\delta \vec{v} = \alpha R \Omega \left(\frac{r}{R}\right)^m \vec{Y}_{mm}^B e^{i\omega t}$$

This expression provides the definition of  $\alpha$  within the convention used here. In spherical coordinates this expression yields the explicit form

$$\delta \vec{v} = \frac{(-1)^m}{2^m m!} \sqrt{\frac{m(2m+1)(2m)!}{4\pi(m+1)}} \alpha R \Omega \cdot \left(\frac{r}{R}\right)^m (\sin\theta)^{m-1} e^{i(m\phi+\omega t)} \left(-i\hat{\theta} + \cos\theta\hat{\phi}\right)$$

where  $\hat{\theta}$  and  $\hat{\phi}$  are unit vectors in polar and azimuthal direction. With this definition and for  $\alpha = 1$  the maximum value, taken at the equator and in direction of  $\hat{\theta}$ , is roughly  $\delta \vec{v}/\vec{v} \approx 0.3$ , so that the approximation breaks down for  $\alpha \gg 1$  since mass shedding will occur for fast spinning stars. The corresponding maximum density fluctuation  $\delta n/\bar{n}$  obtained from eq. (12) is more than an order of magnitude smaller.

In contrast in [2] an alternative convention  $\alpha'$  of the amplitude was introduced that is related to the above  $\alpha$  by

$$\alpha = \sqrt{\frac{\pi(m+1)^3(2m+1)!}{m}} \alpha'$$

i.e. defined by eq. (A1) without the algebraic prefactor.

### Appendix B: Approximate result for strange quark matter

Whereas the bulk viscosity of semi-leptonic processes in hadronic and quark matter require in general a numeric solution, for the dominant contribution from non-leptonic processes in strange quark matter an approximate solution valid in both subthermal and suprathreshold regimes is possible. The approximate analytic result for the bulk viscosity in the suprathreshold regime obtained from a Fourier analysis, is given by [12]

$$\zeta^> \approx \frac{2}{3\sqrt{3}} \frac{C^2}{B\omega} h \left( \frac{9\sqrt{3}\chi}{8} \frac{\tilde{\Gamma} B C^2 T^{\delta-2}}{\omega} \left( \frac{\Delta n_*}{\bar{n}_*} \right)^2 \right) \quad (\text{B1})$$

where  $\chi \equiv \chi_1$  and

$$h(z) = \frac{9}{4z} \left( \left( \sqrt{z^2+1} - z \right)^{\frac{2}{3}} + \left( \sqrt{z^2+1} + z \right)^{\frac{2}{3}} - 2 \right) \quad (\text{B2})$$

A very good parameterization valid in both the sub- and suprathreshold regime is given by [12]

$$\zeta_{par} \approx \zeta^< + \theta(T_{max} - T) \frac{\zeta_{max} - \zeta^<}{\zeta_{max}} \zeta^> \quad (\text{B3})$$

Since the functional form of the suprathreshold viscosity eq. (B2) is still complicated and does not allow to perform the necessary subsequent integrations to obtain the r-mode damping time in an analytic form, we give an approximate analytic result that is valid up to the maximum of the bulk viscosity. To this end we perform a global polynomial interpolation to the function  $h(z)$  in the interval  $[0, z_{max}]$ . In order to appropriately describe the low amplitude behavior and the qualitative form be-

low the maximum requires at least a quartic polynomial which is then uniquely determined as

$$h_{pol}(z) = z - \frac{1}{2\sqrt{3}}z^2 + \frac{1}{27}z^3 - \frac{1}{324\sqrt{3}}z^4 \quad (\text{B4})$$

The leading linear term in eq. (B4) reproduces the approximate intermediate linear result given by Madsen [14], whereas the other terms ensure the proper large amplitude saturation. The analytic form and the polynomial approximation agree in the relevant region below the maximum point-wise on the 5% level and the corresponding integrals required for the damping time to even better accuracy.

The density in a strange star is nearly constant and so the density dependent quantities can be approximated by their value at the radius of the star, denoted by the suffix  $R$ . Performing the integration over the r-mode profile eq. (12), we find the approximate analytic result for the viscous damping time

$$\frac{1}{\tau_B^>} \approx \frac{16}{5103} \frac{A_R^2 C_R^2 \Omega^3 R^5}{B_R M \tilde{J}} \left( \frac{\frac{3}{2} \Omega \tilde{\Gamma}_R B_R T^\delta}{\Omega^2 + \frac{9}{4} \tilde{\Gamma}_R^2 B_R^2 T^{2\delta}} + \frac{2430}{143} \theta(T_{max} - T) \frac{(\Omega - \frac{3}{2} \tilde{\Gamma}_R B_R T^\delta)^2}{\Omega^2 + \frac{9}{4} \tilde{\Gamma}_R^2 B_R^2 T^{2\delta}} g(\chi \tilde{\Gamma}_R A_R^2 B_R C_R^2 R^4 \Omega^3 T^{\delta-2} \alpha^2) \right) \quad (\text{B5})$$

where  $g$  is the polynomial

$$g(x) = x - \frac{151875}{9044}x^2 + \frac{1063125}{7429}x^3 - \frac{290631796875}{587723048}x^4$$

- 
- [1] J. Papaloizou and J. E. Pringle, *Non-radial oscillations of rotating stars and their relevance to the short-period oscillations of cataclysmic variables*, Mon. Not. Roy. Astron. Soc. **182** (1978) 423–442.
- [2] L. Lindblom, G. Mendell, and B. J. Owen, *Second-order rotational effects on the r-modes of neutron stars*, Phys. Rev. **D60** (1999) 064006, [[\ttgr-qc/9902052](#)].
- [3] N. Andersson, *A new class of unstable modes of rotating relativistic stars*, Astrophys. J. **502** (1998) 708–713, [[\ttgr-qc/9706075](#)].
- [4] M. Alford, S. Mahmoodifar, and K. Schwenzer, *Viscous damping of r-modes: Small amplitude instability*, [[\ttarXiv:1012.4883](#)].
- [5] B. J. Owen *et al.*, *Gravitational waves from hot young rapidly rotating neutron stars*, Phys. Rev. **D58** (1998) 084020, [[\ttgr-qc/9804044](#)].
- [6] L. Lindblom, J. E. Tohline, and M. Vallisneri, *Non-Linear Evolution of the r-Modes in Neutron Stars*, Phys. Rev. Lett. **86** (2001) 1152–1155, [[\ttastro-ph/0010653](#)].
- [7] R. Bondarescu, S. A. Teukolsky, and I. Wasserman, *Spin Evolution of Accreting Neutron Stars: Nonlinear Development of the R-mode Instability*, Phys. Rev. **D76** (2007) 064019, [[\ttarXiv:0704.0799](#)].
- [8] P. Arras *et al.*, *Saturation of the r-mode instability*, Astrophys. J. **591** (2003) 1129–1151, [[\ttastro-ph/0202345](#)].
- [9] P. Gressman, L.-M. Lin, W.-M. Suen, N. Stergioulas, and J. L. Friedman, *Nonlinear r-modes in neutron stars: Instability of an unstable mode*, Phys. Rev. **D66** (2002) 041303.
- [10] L.-M. Lin and W.-M. Suen, *Nonlinear r-modes in neutron stars: A hydrodynamical limitation on r-mode amplitudes*, Mon. Not. Roy. Astron. Soc. **370** (2006) 1295–1302, [[\ttgr-qc/0409037](#)].
- [11] L. Bildsten and G. Ushomirsky, *Viscous Boundary-Layer Damping of R-Modes in Neutron Stars*, Astrophys. J. Lett. **529** (Jan., 2000) L33–L36, [[\ttastro-ph/](#)].
- [12] M. G. Alford, S. Mahmoodifar, and K. Schwenzer, *Large*

- amplitude behavior of the bulk viscosity of dense matter, *J. Phys.* **G37** (2010) 125202, [[\ttarXiv:1005.3769](#)].
- [13] A. Reisenegger and A. A. Bonacic, *Bulk viscosity,  $r$ -modes, and the early evolution of neutron stars*, [[\ttastro-ph/0303454](#)].
- [14] J. Madsen, *Bulk viscosity of strange dark matter, damping of quark star vibration, and the maximum rotation rate of pulsars*, *Phys. Rev.* **D46** (1992) 3290–3295.
- [15] I. A. Shovkovy and X. Wang, *Bulk viscosity in nonlinear and anharmonic regime of strange quark matter*, [[\ttarXiv:1012.0354](#)].
- [16] P. Demorest, T. Pennucci, S. Ransom, M. Roberts, and J. Hessels, *Shapiro delay measurement of a two solar mass neutron star*, *Nature* **467** (2010) 1081–1083, [[\ttarXiv:1010.5788](#)].
- [17] F. Özel, D. Psaltis, S. Ransom, P. Demorest, and M. Alford, *The Massive Pulsar PSR J1614-2230: Linking Quantum Chromodynamics, Gamma-ray Bursts, and Gravitational Wave Astronomy*, *Astrophys. J. Lett.* **724** (Dec., 2010) L199–L202, [[\ttarXiv:1010.5790](#)].
- [18] M. Alford, S. Mahmoodifar, and K. Schwenzer, *Non-linear viscous saturation of  $r$ -modes*, [[\ttarXiv:1012.4834](#)].
- [19] M. G. Alford, S. Mahmoodifar, and K. Schwenzer, *Suprathermal viscosity of dense matter*, [[\ttarXiv:1009.4182](#)].
- [20] E. Witten, *Cosmic Separation of Phases*, *Phys. Rev.* **D30** (1984) 272–285.
- [21] A. Akmal, V. R. Pandharipande, and D. G. Ravenhall, *The equation of state for nucleon matter and neutron star structure*, *Phys. Rev.* **C58** (1998) 1804–1828, [[\ttnucl-th/9804027](#)].
- [22] G. Baym, C. Pethick, and P. Sutherland, *The Ground state of matter at high densities: Equation of state and stellar models*, *Astrophys. J.* **170** (1971) 299–317.
- [23] J. W. Negele and D. Vautherin, *Neutron star matter at subnuclear densities*, *Nucl. Phys.* **A207** (1973) 298–320.
- [24] J. M. Lattimer, M. Prakash, C. J. Pethick, and P. Haensel, *Direct URCA process in neutron stars*, *Phys. Rev. Lett.* **66** (1991) 2701–2704.
- [25] B. L. Friman and O. V. Maxwell, *Neutron Star Neutrino Emissivities*, *Astrophys. J.* **232** (1979) 541–557.
- [26] R. F. Sawyer, *Bulk viscosity of hot neutron-star matter and the maximum rotation rates of neutron stars*, *Phys. Rev.* **D39** (1989) 3804–3806.
- [27] A. Reisenegger, *Deviations from chemical equilibrium due to spindown as an internal heat source in neutron stars*, *Astrophys. J.* **442** (1995) 749, [[\ttastro-ph/9410035](#)].
- [28] P. Haensel and R. Schaeffer, *Bulk viscosity of hot-neutron-star matter from direct URCA processes*, *Phys. Rev.* **D45** (1992) 4708–4712.
- [29] P. S. Shternin and D. G. Yakovlev, *Shear viscosity in neutron star cores*, *Phys. Rev.* **D78** (2008) 063006, [[\ttarXiv:0808.2018](#)].
- [30] M. Alford, M. Braby, M. W. Paris, and S. Reddy, *Hybrid stars that masquerade as neutron stars*, *Astrophys. J.* **629** (2005) 969–978, [[\ttnucl-th/0411016](#)].
- [31] H. Heiselberg and C. J. Pethick, *Transport and relaxation in degenerate quark plasmas*, *Phys. Rev.* **D48** (1993) 2916–2928.
- [32] H. Heiselberg, *The Weak conversion rate in quark matter*, *Phys. Scripta* **46** (1992) 485–488.
- [33] R. C. Tolman, *Static solutions of Einstein’s field equations for spheres of fluid*, *Phys. Rev.* **55** (1939) 364–373.
- [34] L. Lindblom, B. J. Owen, and S. M. Morsink, *Gravitational radiation instability in hot young neutron stars*, *Phys. Rev. Lett.* **80** (1998) 4843–4846, [[\ttgr-qc/9803053](#)].
- [35] N. Chamel and P. Haensel, *Physics of Neutron Star Crusts*, *Living Rev. Rel.* **11** (2008) 10, [[\ttarXiv:0812.3955](#)].
- [36] A. A. Bonacic, *Gravitational radiation and bulk viscosity in neutron stars*, Master thesis, Universidad Catolica de Chile (2003).
- [37] L. Lindblom and B. J. Owen, *Effect of hyperon bulk viscosity on neutron-star  $r$ - modes*, *Phys. Rev.* **D65** (2002) 063006, [[\ttastro-ph/0110558](#)].
- [38] M. G. Alford, S. Reddy, and K. Schwenzer, *Bridging the gap by shaking superfluid matter*, [[\ttarXiv:1110.6213](#)].
- [39] J. Brink, S. A. Teukolsky, and I. Wasserman, *Nonlinear couplings of  $R$ -modes: Energy transfer and saturation amplitudes at realistic timescales*, *Phys. Rev.* **D70** (2004) 121501, [[\ttgr-qc/0406085](#)].
- [40] R. Bondarescu, S. A. Teukolsky, and I. Wasserman, *Spinning down newborn neutron stars: nonlinear development of the  $r$ -mode instability*, *Phys. Rev.* **D79** (2009) 104003, [[\ttarXiv:0809.3448](#)].
- [41] J. Madsen, *How to identify a strange star*, *Phys. Rev. Lett.* **81** (1998) 3311–3314, [[\ttastro-ph/9806032](#)].
- [42] N. Andersson, D. I. Jones, and K. D. Kokkotas, *Strange stars as persistent sources of gravitational waves*, *Mon. Not. Roy. Astron. Soc.* **337** (2002) 1224, [[\ttastro-ph/0111582](#)].
- [43] A. Drago, G. Pagliara, and I. Parenti, *A compact star rotating at 1122 Hz and the  $r$ -mode instability*, *Astrophys. J.* **678** (2008) L117–L120, [[\ttarXiv:0704.1510](#)].
- [44] M. Prakash *et. al.*, *Composition and Structure of Protoneutron Stars*, *Phys. Rept.* **280** (1997) 1–77, [[\ttnucl-th/9603042](#)].
- [45] R. N. Manchester, G. B. Hobbs, A. Teoh, and M. Hobbs, *The ATNF Pulsar Catalogue*, *Astron. J.* **129** (2005) 1993, [[\ttastro-ph/0412641](#)].
- [46] A. Reisenegger and A. A. Bonacic, *Millisecond pulsars with  $r$ -modes as steady gravitational radiators*, *Phys. Rev. Lett.* **91** (2003) 201103, [[\ttastro-ph/0303375](#)].
- [47] J. R. Ipser and L. Lindblom, *Oscillations and stability of rapidly rotating neutron stars*, *Phys. Rev. Lett.* **62** (1989) 2777–2780.
- [48] We note that we had previously used the alternative  $\alpha$ -definition [2] in the proceedings article [18] and a preprint version of the present article, which led to lower values for the saturation amplitudes, see also Appendix A.
- [49] The range  $n_0/4$  to  $n_0/2$  should provide an estimate for the uncertainty of this boundary. For instance in [35] an intermediate value of  $n_0/3$  is given.